APPROACHING ATOMIC RESOLUTION IN CRYSTALLOGRAPHY OF RIBOSOMES

Ada Yonath

Department of Structural Biology, Weizmann Institute, Rehovot, Israel, and Max-Planck-Research-Unit for Ribosomal Structure, Hamburg, Germany

CONTENTS

77

PERSPECTIVES AND OVERVIEW

The translation of the genetic code into proteins is facilitated by a universal cellular organelle, the ribosome. The fundamental significance of the ribosome triggered intensive studies that led to important advancements: the determination of the primary sequences of many ribosomal components; sound propositions for the secondary structures of the rRNA chains; suggestions for spatial proximities between several ribosomal components; an insight into aspects in evolution; elaborate genetic manipulations; approximations of the size and the shape of the ribosome; and a fairly detailed description of the overall process of protein biosynthesis. At the same time these studies showed that a reliable molecular model of the ribosome is a prerequisite for the determination of the mechanism of protein biosynthesis.

The ribosome is an assembly of proteins and RNA chains. A typical bacterial ribosome contains some 56 different proteins and three RNA chains weighing a total of 2.3 million daltons. This assembly is unstable, flexible, and possesses no internal symmetry, and therefore is considered a rather complicated object for crystallographic analysis. Even its crystallization was believed to be a formidable task. However, natural in vivo organizations of eukaryotic ribosomes in periodic structures were detected in organisms exposed to stressful conditions, such as suboptimal temperatures, wrong diet, or lack of oxygen (for review see 42). The existence of these ordered formations stimulated extensive attempts to grow three-dimensional crystals of prokaryotic ribosomes. These were chosen because they are well characterized biochemically and may provide systems for in vitro crystallization, independent of in vivo events, environmental influences, and physiological factors that might be difficult or impossible to control and to reproduce.

As a result, natural and mutated 70S ribosomes and their small (30S) and large (50S) subunits were crystallized. Quality crystals were also obtained from chemically modified (with heavy atom clusters) particles and from complexes, which mimicked defined functional states in protein biosynthesis (Table 1). To facilitate subsequent crystallographic analysis, novel procedures for data collection and for derivatization have been established and low resolution images have been reconstructed.

This chapter describes the initial, intermediate, and current states of the structural studies of ribosomes. The crystallographic work with both X-rays and neutrons is addressed and the results obtained through image reconstructions from ordered arrays are compared with those derived from investigations of single particles. The review highlights the influence of structural results on subsequent functional studies and the contribu-

Table 1 Characterized three-dimensional crystals of ribosomal particles

Source[a]	Grown form	Cell dimensions (Å)	Resolution (Å)[b]
70S T.t.	MPD[c]	$524 \times 524 \times 306$; $P4_12_12$	approx. 20
70S T.t.+			
m-RNA & t-RNA[d]	MPD	$524 \times 524 \times 306$; $P4_12_12$	approx. 15
30S T.t.	MPD	$407 \times 407 \times 170$; $P42_12$	7.3
50S H.m.	PEG[c]	$210 \times 300 \times 581$; $C222_1$	3.0
50S T.t.	AS[c]	$495 \times 495 \times 196$; $P4_12_12$	8.7
50S B.st.[e]	A[c]	$360 \times 680 \times 920$; $P2_12_12$	approx. 18
50S B.st.[e,f]	PEG	$308 \times 562 \times 395$; $114°$; C2	approx. 11

[a] B.st., *Bacillus stearothermophilus*; T.t., *Thermus thermophilus*; H.m., *Haloarcula marismortui*.

[b] Represents the highest resolution for which sharp diffraction spots could be consistently observed. In many instances, we could not collect useful crystallographic data to this resolution.

[c] MPD, PEG, A, AS = crystals grown by vapor diffusion in hanging drops from solutions containing methyl-pentane-diol (MPD), polyethyleneglycol (PEG), ammonium sulphate (AS), or low molecular weight alcohols (A).

[d] A complex including 70S ribosomes, two equivalents of PhetRNA^Phe and an oligomer of 35 ± 5 uridines, serving as mRNA.

[e] Same form and parameters for crystals of large ribosomal subunits of a mutant (missing protein BL11) of the same source and for modified particles with an undecagold-cluster.

[f] Same form and parameters for crystals of a complex of 50S subunits, one tRNA molecule and a segment (18–20 mers) of a nascent polypeptide chain.

tion of biochemical experiments to the progress of the crystallographic work.

THE INITIAL STAGES: OBTAINING CRYSTALS

Choosing Halophilic and Thermophilic Prokaryotic Ribosomes

The key for obtaining diffracting crystals was the choice of the appropriate organism. The initial targets for crystallization were the ribosomes from *Escherichia coli* as they are fully characterized biochemically. Because these ribosomes are rather sensitive and unstable, only small two-dimensional arrays (24) or micro three-dimensional crystals (41) could be grown from them. Consequent extensive screening efforts showed that the most suitable sources for crystallizable ribosomes are extreme halophilic and thermophilic bacteria, probably because these ribosomes are rather stable.

The 50S subunits of the moderate thermophile, *Bacillus stearothermophilus*, were the first ribosomal particles to be crystallized (47). Although the initially grown micro-crystals were not suitable for crystallographic analysis, they played a crucial role in the progress of ribosomal crystallography because their diffraction patterns contained features to 3.5-Å resolution, with spacings compatible with those obtained from gels

of prokaryotic ribosomes (20). Seven crystal forms of 50S subunits, one of 30S subunits, and one of whole 70S ribosomes were grown from these bacteria under a variety of conditions (43). Among them, the two forms suitable for medium-resolution studies (Table 1) (30) may provide unique information, because they could be specifically derivatized, using mutagenesis, with a multi heavy-atom cluster (see below) (39).

The ribosomes of the archaebacterium, *Haloarcula marismortui* (previously called *Halobacterium marismortui* or *Halobacterium* of the Dead Sea), maintain their integrity, stability, and biological functioning under high salt concentrations, conditions that usually cause denaturation of proteins and dissociation of protein assemblies with nucleic acids. Therefore these ribosomes provide a system suitable for crystallization under most favorable conditions. Furthermore, the determination of their structure should not only illuminate the process of protein biosynthesis, but also may reveal some factors governing the formation of assemblies of nucleic acid with protein. Five crystal forms of 50S subunits and one of the 30S subunits from this bacterium were grown; one of them diffracts to the highest resolution obtained so far, 3 Å (Figure 1, Table 1) (26, 37a).

The ribosomes of the extreme thermophile *Thermus thermophilus* are currently being characterized biochemically in several laboratories because of the growing interest in thermal stability of biological macromolecules. The 70S ribosomes of this bacterium were crystallized in two similar, however not identical, forms (35, 36, 43). Diffracting crystals were also obtained from 30S (44) and 50S subunits (37) as well as from complexes of 70S ribosomes with mRNA and tRNA (14). Thus, structural analysis of the crystalline ribosomal particles from this bacterium (Table 1) should provide information concerning conformational changes correlated with selected steps in the process of protein biosynthesis.

Several common properties have been observed in crystallization of prokaryotic ribosomal particles, regardless of their source. Functional activity is a prerequisite for crystal growth, but not every active preparation yields high quality crystals. Thus, it seems that the requirements for crystallization are more severe than those for biological activity, and extreme care in growing the cells and in the preparation of the ribosomes is necessary for obtaining crystallizable particles. It was found that the basic factors governing the quality of crystals are related more to the quality of the ribosomal particles than to choice of the crystallizing agent (49); however, the exact conditions for the growth of quality crystals must still be refined for each preparation. In all cases, the crystallized material retains its integrity and biological activity for long periods, in contrast to the short lifetime of isolated ribosomes.

Several Aspects of Nucleation and Crystal Growth

As ribosomes are large enough to be seen using electron microscopy, some steps in the nucleation and in the growth of ribosome crystals could be directly observed (45). It was observed that under proper crystallization conditions, the process of crystal growth starts within the first few hours by nonspecific aggregation, which is likely to inhibit the natural tendency of ribosomes to disintegrate. These amorphous aggregates undergo rearrangements toward the formation of nuclei of different morphologies, including star-shaped crystallites and various helical arrangements. These organizations may explain the extreme sensitivity of the crystallization process to small changes in external conditions and the commonly observed high mosaicity. Thus, it is not surprising that several different crystal forms were developed under similar conditions, and that small variations in the growth media introduced large differences in the crystallographic constants (e.g. the presence of 0.2 M KCl caused a change of 65 Å in the length of one axis of the crystals of 70S ribosomes from *T. thermophilous*) (36, 43).

In general, Mg^{2+} plays an essential role in maintaining the integrity of ribosomes. Our studies showed that it is also most crucial for their crystallization. For example, in spontaneous crystallization of several crystal types, the lower the Mg^{2+} concentration is, the thicker the crystals are. Interestingly, the upper critical value of Mg^{2+} permitted for the growth of three-dimensional crystals of 50S from *B. stearothermophilus* is the lowest needed for obtaining two-dimensional arrays (1).

The optimal conditions for the crystallization of halophilic ribosomes were established according to the complementary effects of mono and divalent ions. Mild variations in the delicate equilibrium of these ions enabled the development of a sophisticated seeding procedure (26, 49). Subsequent studies led to the establishment of a procedure that allows the crystallization of the halophilic ribosomes at the lowest concentrations of salts essential to maintain their integrity and the collection of diffraction data from crystals soaked in solutions mimicking their physiological environment.

Minute quantities of additives, such as metal ions with a high coordination of organic materials with a low surface tension, dramatically influenced the appearance or the quality or the morphology of several crystal types, in accord with observations obtained for isolated proteins (28). In particular, the addition of 1 mM Cd^{2+} to the growth media of 50S subunits from *H. marismortui* resulted in crystals diffracting to 3-Å resolution, with reasonable mosaicity and superb mechanical stability (37a).
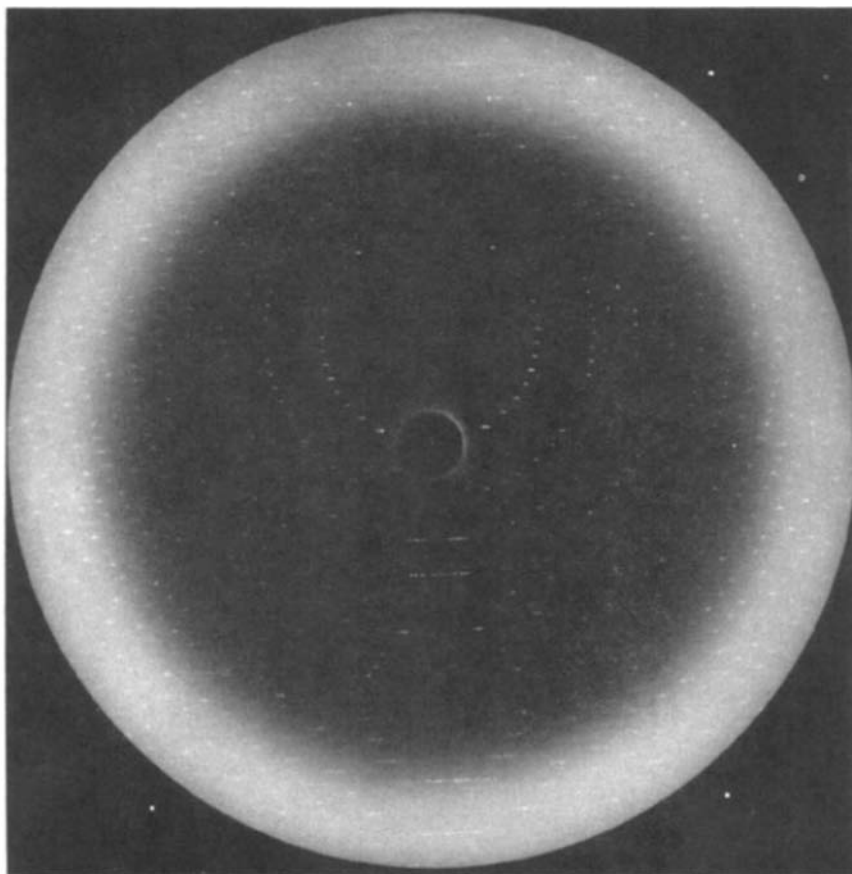
Figure 1 Rotation photograph of a crystal of 50S ribosomal subunits from *H. marismortui* grown by vapor diffusion in Linbro dishes coupled with individual seeding at 19°C from 6–8 μl of: 5 mg/ml 50S subunits, 1.2 M potassium chloride, 0.5 M ammonium chloride, 0.005 M magnesium chloride, 0.001 M cadmium chloride, and 5–6% polyethyleneglycol (6000), at pH 5.6 equilibrated with 1 ml reservoir of 1.7 M KCl and all the other components of the drop. The crystal was kept in 3 M potassium chloride, 0.5 M ammonium chloride, 0.005 M magnesium chloride, 0.001 M cadmium chloride, and 8% polyethyleneglycol (6000) at pH 5.6. Before cooling, it was soaked for 15 minutes in a solution containing the above storage components and 18% ethyleneglycol. The pattern was obtained at 90 K at Station F1/CHESS, operating at about 5.3 Gev and 50–80 mA. The crystal to film distance was 220 mm, the diameter of the collimator = 0.1 mm; wave length = 0.9091 Å.

# INTERMEDIATE RESULTS: RECONSTRUCTED MODELS AT LOW RESOLUTION

Electron Microscopy of Sectioned Three-Dimensional Crystals

Some of the naturally occurring eukaryotic periodic organizations (see Perspectives and Overview) enabled image reconstruction studies that yielded low resolution information about the interactions between the particles, the outer contour of the ribosome, and the inner distribution of its components (for review, see 42). Similar procedures were employed for the analysis of the initially obtained three-dimensional crystals from prokaryotic sources. These were too small for X-ray or neutron crystallography, but too thick for direct investigation using electron microscopy. Therefore, positively stained thin sections of cross-linked and embedded crystals were investigated. Such analysis is limited by the inherent lower resolution induced by the embedding process, by the uncertainty regarding the exact sectioning direction, and by the unknown factors governing the stain distribution within the particle. However, despite these shortcomings, useful information could be extracted concerning the packing of the crystals of the 70S ribosome from *E. coli* (41) and the stain-distribution within the 50S subunits from *B. stearothermophilus*. The latter was obtained through three-dimensional reconstructions using four different crystal forms at a very low resolution, 60–90 Å. The resulting models, built of two domains of unevenly distributed density (25), were strikingly similar to models obtained a few years later at significantly higher resolution, 28 Å, from two-dimensional arrays (Figure 2) grown under different crystallization conditions and exposed to radically different experimental treatments (46).

Image Reconstruction from Two-Dimensional Arrays

Investigations of negatively stained isolated ribosomes using electron microscopy, coupled with immunology, performed in many laboratories, led to the estimation of the sizes and the shapes of the ribosomal particles and to suggestions for possible locations of several ribosomal components (for review, see 15, 17). Two-dimensional ordered arrays differ fundamentally from single particles in their suitability for image reconstruction in three dimensions. Based on diffraction data, rather than on averaging of selected particles, the reconstruction is inherently more objective. In addition, the particles in the two-dimensional arrays are held by lattice forces, which may reduce structural deformations caused by the contacts of the particles with the flat microscopical grids.

The growth of the first two-dimensional arrays of bacterial ribosomal particles was reported over a decade ago (24). A few years later these
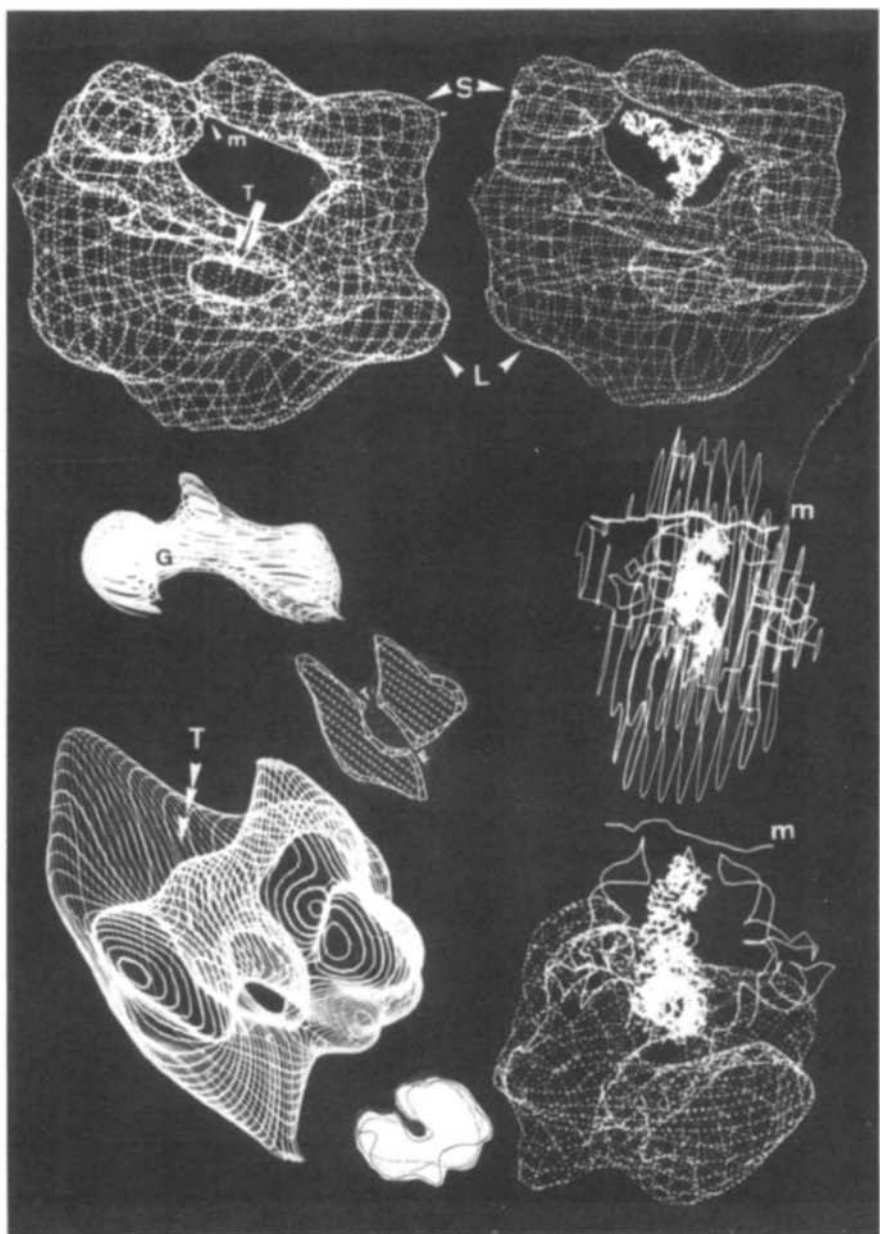
alcohol-grown arrays of ribosomal subunits from *E. coli* reached a size marginally suitable for image reconstruction (8, 31). The initial two-dimensional arrays of 50S subunits from *B. stearothermophilus* were also obtained from alcohols by employing essentially the same crystallization conditions used for the growth of three-dimensional crystals of these particles (47) while increasing the relative Mg^{2+} concentrations (1). The second-generation arrays, obtained a few years later, were grown within less than 1 min, directly on electron microscopy grids using salt-alcohol mixtures. Tilt series of two-dimensional arrays of 70S ribosomes and 50S subunits of *B. stearothermophilus*, negatively stained with gold thioglucose, led to reconstructed images at 47 and 28 Å, respectively (Figure 2) (2, 46). These showed several key features, associated mainly with internal vacant spaces or partially filled hollows, that were not detected earlier. The significant similarities in the overall shapes and in several specific features of corresponding regions in several reconstructed models allowed the assessment of their reliability, the location of the 50S subunit within the 70S ribosome, the extraction of an approximate model for associated 30S subunits, and the tentative assignment of biological functions to several structural features (Figure 2) (43, 50). However, an accurate determination of the shape and the size of the ribosome, as well as a detailed assignment of its functional sites, still awaits higher resolution data.

Figure 2 Computer-graphic displays of models obtained by three-dimensional reconstructions of 70S ribosomes (at 47-Å resolution) and 50S ribosomal subunits (at 28-Å resolution) of *B. stearothermophilus*, from tilt series of negatively stained (with gold-thioglucose) two-dimensional arrays, viewed using electron microcopy. S and L mark the small and the large subunits, respectively. T shows the entrance to the tunnel and E its exit. G marks the groove in the small subunit, presumed to be the path of m, the mRNA.

(*Top left*) The 70S ribosome, shown as a net.

(*Bottom left*) The 50S subunit, shown in fine lines. Inserts: (*upper right corner*) a slice of 20-Å thickness of this subunit; (*bottom right corner*) the reconstructed stain density from positively stained thin sections of three-dimensional micro crystals from the same source.

(*Middle left*) The shape of the 30S subunit as obtained by subtracting the density of the 50S subunit from that of the 70S ribosome.

(*Top right*) A tRNA molecule, positioned by model building in the intersubunit free space in the 70S ribosome (*top left*).

(*Middle right*) A perpendicular view of the model shown in top right. The ribosome is outlined by vertical lines. Fitted into the intersubunit space of the ribosome by model building are the backbones of a chain of 28 nucleotides in an arbitrary conformation, and of two molecules of tRNA. The third tRNA shown in the middle is highlighted by including all its atoms (as in top right).

(*Bottom right*) The 50S subunit in the same orientation as it is in the ribosome shown in the middle right panel, together with the components included by model building. The outline of the whole ribosome was removed for clarity.

POSSIBLE FUNCTIONAL RELEVANCES IN THE RECONSTRUCTED MODELS

Approximate Shapes of the Ribosomal Subunits Within the Assembled 70S Ribosome

Based on common structural elements, the reconstructed model of the isolated 50S subunit was fitted into that of the 70S ribosome. The overall agreement in the shapes of the reconstructed isolated 50S subunit and the part of the ribosome it was assigned to is quite striking. The few slight differences, detected mainly in two regions, one of which is close to the subunit interface, may reflect conformational changes occurring upon the association of the subunits, or resulting from the differences in the resolutions of the two reconstructions (5).

The approximate shape of the associated 30S subunit was deduced by subtracting the part assigned as the 50S subunit from the model of the whole ribosome (Figure 2). There is a significant similarity in the volumes and in the overall shapes of isolated (for review, see 15, 17) and bound 30S subunits, but the isolated particles appear somewhat wider than those extracted from the assembled ribosome. Flattening of isolated 30S particles on the microscopic grids may account for these differences. Such deformations are virtually eliminated in the two-dimensional arrays used for the reconstruction of the assembled ribosomes, because in these arrays, most of the contacts of the ribosomes with the electron microscopical grids are through the 50S subunits. Alternatively, the differences could result from conformational changes of the 30S subunits upon their incorporation into the ribosome.

Tentative Assignments for the Path of the Nascent Proteins and for the Site for the Biosynthetic Reaction

A prominent feature in the reconstructed models of both 70S ribosomes and 50S subunits is a tunnel spanning the 50S subunit of about 100 Å in length and up to 25 Å in diameter (Figure 2) (46). A tunnel within the large ribosomal subunit was predicted more than two decades ago, when it was shown that the ribosome masks the latest synthesized segments of nascent chains (27). This tunnel may be the path of the newly synthesized proteins because it leads from the intersubunit space, which was presumed to be the peptidyl transferase site (see below), to a location that may be compatible with that suggested as the site for the emerging nascent polypeptide by immuno electron microscopy experiments (4). A similar feature was also apparent in image-reconstructed 80S eukaryotic ribo-

somes (29) and in neutron diffraction maps of 50S subunits of *H. maris-mortui* (10). The current resolution does not permit an accurate determination of the diameter of the tunnel. However, the tunnel seems spacious enough to impose no restrictions to the sequence of the growing peptides and may accommodate amino acids to which bulky groups, such as biotin, have been bound (23). In recent immuno electron microscopy experiments, the N-termini of nascent chains were detected in two locations: one close to the subunit interface, where the end of short polypeptides were detected, and the second at the other end of the particle (34), where the N-termini of longer chains were found. Further studies indicated that ribosomes protect natural proteins more efficiently than artificial homopolymers (21) and that the latter may choose a path slightly different from that chosen by naturally occurring proteins (16).

Thus, it seems that the amino termini of natural proteins have a common feature that guides nascent chains into the tunnel. Homopolypeptides lacking this feature may miss the entrance to the tunnel. Thus, the differences in the migration of short and long chains of polyphenylalanine and polylysine (16) may be correlated with a mechanism in which newly formed peptides that hit the correct exit path continue to grow and migrate normally out of the ribosome, whereas those that miss the tunnel adhere to the surface of the ribosome and cause early termination of the biosynthetic pathway. This hypothesis may explain why only 40–60% of most ribosomal preparations are found to be active in the synthesis of relatively long polypeptides, although almost all well-prepared ribosomes bind mRNA and tRNA (14, 32). In fact under some conditions, short nascent homopolypeptides adhere to ribosomes of *E. coli* (13). Furthermore, complexes of short chains of polyphenylalanine or polylysine with 50S subunits from *B. stearothermophilus* and *H. marismortui* were crystallized (43).

The small and large ribosomal subunits are well separated in most reconstructions of whole ribosomes, regardless of the source of the ribosome, the staining material, and the computational treatments (2, 11, 29, 38, 50). An empty space, comprising about 20% of the volume of the ribosome, located at the interphase between the two ribosomal subunits was clearly resolved in reconstructed images of 70S ribosomes from *B. stearothermophilus* (Figure 2) (50). This space may provide the flexibility, dynamics, and the mobility needed for the process of protein biosynthesis. Volume calculations showed that it is large enough to accommodate up to three tRNA molecules together with other factors participating in this process. Therefore it was tentatively assigned as the site of protein biosynthesis.

Regions rich in rRNA were detected through preferential staining of the two-dimensional arrays, in several locations on the walls of the free space, one of them in the vicinity of a groove in the 30S subunit (50). In accord with biochemical evidence and modeling experiments (7), this groove was tentatively assigned as the path of the mRNA chain. In a model-building experiment, a molecule of tRNA was placed in the intersubunit space with its anticodon close to the tentative mRNA binding site and its CCA-terminus positioned so that the peptidyl group could extend into the tunnel (Figure 2) (43, 50). In this orientation, the tRNA interacts at many sites with the walls of the intersubunit space. These interactions may account for noncognate affinity of the tRNA to the ribosome and provide a mechanism for communication between the path of the nascent chain and the decoding region.

Crystallizable Complexes Mimicking Defined Functional States

The characteristic low resolution of all crystals of whole ribosomes obtained so far may be related to the inherent conformational heterogeneity of their preparations. Reassembled ribosomes from purified 50S and 30S subunits, which are expected to be fairly homogenous, yielded crystals containing solely the 50S subunits (14), showing that the interparticle interactions in the crystals of the 50S subunits are stronger than the affinity between the large and small subunits in 70S particles kept for long periods without having the opportunity to participate in protein biosynthesis. This experiment highlights the readiness of the large ribosomal subunits to crystallize, a property also reflected by the large number of crystal forms obtained from these particles (26, 30, 37, 37a, 42, 43, 47, 48). It also is in accord with observations made on two-dimensional arrays of 80S ribosomes, which showed that these arrays could be depleted of the small subunits and still maintain their packing integrity (22).

To minimize the flexibility of the ribosomes and to increase the homogeneity of the crystallized material, complexes were prepared that mimicked defined stages in protein biosynthesis. A model complex of 70S ribosomes from *T. thermophilus* with two equivalents of phetRNA[phe] and a chain of about 35 uridyl residues was first crystallized. The reproducibility of the growth of crystals and their internal order dramatically improved (Table 1) (14). To assess the individual contributions of the different components to the stability of this complex, 70S ribosomes were cocrystallized together with a chain of 35 uridines. Only poorly shaped crystals were occasionally grown, indicating the larger contribution of the tRNA molecule to the stability of this system.

CURRENT CRYSTALLOGRAPHIC ANALYSIS

X-Ray Data Collection with Synchrotron Radiation at Cryotemperature

The diffracting power of crystalline ribosomal particles is so weak that synchrotron radiation is required for virtually all the crystallographic studies. At ambient temperatures, the radiation damage of the ribosomal crystals is so rapid that all reflections beyond approximately 15–18 Å decay within a few minutes, a period shorter than the time required to obtain a single useful X-ray pattern. This severe decay led to underestimation of the real resolution, to occasional assignment of wrong unit cell constants, and to unsuccessful attempts to collect complete diffraction data sets. Only the pioneering introduction of a procedure for crystallography at cryogenic temperature enabled productive studies. Thus, shock-frozen, irradiated crystals measured surrounded by a nitrogen stream at about 90 K did not show radiation damage over long periods, enabling the collection of complete diffraction data sets from individual crystals (18).

All ribosomal crystals could be measured at cryotemperature, although a thorough search to establish individual freezing conditions for each crystal form was essential. This work revealed that the resolution limits and the mosaicity obtained at cryotemperatures from ribosomal crystals equaled those obtained at ambient temperature. However, as there is practically no time limit for irradiation at cryotemperature, the reflections with the highest resolution, which are usually the weakest, could be detected. Comparisons of diffraction data collected at intervals of 0.5, 2, and 153 days from the same crystal showed no significant differences in the intensities or in the cell parameters.

Attempts at Phasing

Fourier summation, the operation leading from diffraction patterns to electron density maps, requires information about the direction, amplitude, and phase of each reflection. The directions and amplitudes can be measured, whereas the phases have to be determined indirectly. The most common method for extracting phases in crystallography of macromolecules is multiple isomorphous replacement (MIR). This method involves the introduction of electron-dense atoms to the crystalline lattice at distinct locations, causing measurable changes in the diffraction pattern, while keeping the crystal isomorphous with that of the native molecule. For proteins of average size, useful isomorphous derivatives are obtained using one or a few heavy-metal atoms. Because of the large size of the

ribosome, compact clusters of a proportionally larger number of heavy atoms should be used for its derivatization.

To maximize the extent of derivatization, sophisticated synthetic procedures were developed. An undecagold cluster, consisting of a compact core of eleven gold atoms linked directly to one another (19), was prepared as a monofunctional reagent, specific for sulfhydryl groups (39). As the core of the undecagold cluster is about 8.2 Å in diameter, it can be treated as a single scatterer at low to medium resolution. At this resolution, the structural ambiguities in the location of the reactive moiety on the cluster are negligible. To enhance the accessibility of this bulky cluster, its functional arm was extended with aliphatic chains of varying lengths. A spacer of about 10 Å was needed for efficient binding of the cluster to ribosomal particles, isolated ribosomal components, or modified tRNA molecules. The yield and the specificity of cluster binding to the ribosomal particles was optimized by minimizing the number of exposed sulfhydryl moieties. In this way, the 70S ribosome and the 30S subunits of *T. thermophilus* (43) were fully derivatized without impairing their integrity and their ability to crystallize.

However, direct binding of the cluster to intact ribosomal particles cannot be fully controlled. Therefore, whenever applicable, the cluster was bound to free sulfhydryl moieties of isolated ribosomal components. These were, in turn, reconstituted into core particles. In this way, modified 50S subunits were formed by the binding of the gold cluster to isolated protein BL11 and the incorporation of the cluster-bound protein into cores of mutated ribosomes from *B. stearothermophilus* lacking this protein (39). X-ray diffraction data, of a quality comparable to that of native crystals, were collected from crystals of the modified particles, and the resulting difference Patterson maps included features that could be interpreted as the bound cluster.

Selected proteins can be removed quantitatively from eubacterial ribosomes through mutagenesis (9) or stepwise addition of salts (3). The significant resistance of the halophilic ribosomes to mutations dictates almost exclusively in vitro selective detachment of ribosomal proteins, but at the same time, the high salinity required for the integrity of halophilic ribosomes does not allow substantial alterations. However, treatment with dioxane enabled quantitative removal of several proteins from ribosomes of *H. marismortui*, all of which could be reconstituted quantitatively into core particle. One of the removed proteins, HL11, quantitatively binds reagents specific to sulfhydryls. However, in contrast to protein BL11 from *B. stearothermophilus*, which was reconstituted into core particles even when a group as large as the gold cluster was bound to it, the modified halophilic protein HL11 reconstitutes only when its sulfhydryl group is

free. Even binding of small organic compounds to the sulfhydryl of the isolated protein prevented its association with core particles. Using this property, we could prepare halophilic 50S core particles quantitatively depleted of protein HL11. These were crystallized under the same conditions as that used for native 50S subunits, indicating that the removal of this protein did not cause conformational changes of the 50S subunit.

Obvious carriers for indirect derivatization are tRNA and mRNA. Conditions for stoichiometric binding of tRNA to several ribosomal particles were determined, and complexes that contain tRNA molecules have been crystallized (12, 14, 43). For the derivatization of these complexes, the gold cluster was chemically attached to the X base (at position 47) of tRNAphe from *E. coli*. The modified tRNA molecule could be charged with its cognate amino acid and attached to 70S ribosomes and to 30S ribosomal subunits, in the presence or absence of mRNA, under the same conditions and with the same stoichiometry as native tRNA (S. Weinstein, F. Franceschi, C. Glotz, T. Boeck, M. Laschever & A. Yonath, unpublished data).

A different approach for phasing at low resolution is the use of the reconstructed models in several variations of the molecular replacement method. These procedures are based on the positioning of approximate models of the studied object in the crystallographic unit cells. Such attempts may yield valuable intermediate information concerning mainly the packing of the crystals. To facilitate these studies, crystallographic data for 70S ribosomes from *T. thermophilus* and for 50S subunits from *H. marismortui* and *T. thermophilus* were used together with the models of these particles from *B. stearothermophilus* (see Intermediate Results, above), assuming that prokaryotic ribosomes are of similar structures at low resolution.

Parallel studies have been performed using single crystal neutron diffraction accompanied by contrast variation. This method has already provided useful phasing information, as well as hints about the internal distribution of different components for large cellular assemblies (e.g. 33; reviewed in 10). Neutron diffraction data to 30-Å resolution were collected from crystals of 50S ribosomal subunits from *H. marismortui*. Phased using direct methods, these data led to a relatively clean map, which contained several compact features with a shape similar to that obtained by image reconstruction of the large subunit from *B. stearothermophilus* (10).

CONCLUDING REMARKS

This article demonstrates that crystallographic studies on intact ribosomal particles are feasible, despite the facts that a straightforward application

of conventional macromolecular crystallographic techniques was not
adequate and considerable effort had to be invested in developing con-
ceptual and experimental procedures. Of special significance are the devel-
opment of innovative procedures for crystallization and seeding, the intro-
duction of cryotemperature techniques, and the sophisticated extension of
existing evaluation techniques. Also, the combination of metalo-organic
biochemistry, genetic manipulations, and functional studies enabled spe-
cific labeling of the crystals of the ribosomal particles and of their com-
plexes, without introducing major changes in their crystallizability, integ-
rity, or biological activity. In addition, the interplay with other diffraction
methods, such as neutron crystallography and three-dimensional image
reconstructions from two-dimensional arrays investigated using electron
microscopy led to the elucidation of medium-resolution models, to the
tentative assignments of several functional sites, and to the design of
subsequent functional and structural experiments.

Literature Cited

1. Arad, T., Leonard, K. R., Wittmann, H.
   G., Yonath, A. 1984. *EMBO J.* 3: 127
2. Arad, T., Piefke, J., Weinstein, S.,
   Gewitz, H. S., Yonath, A., Wittmann,
   H. G. 1988. *Biochimie* 69: 1001
3. Atsmon, A., Spitnik-Elson, P., Elson, D.
   1969. *J. Mol. Biol.* 45: 125
4. Barnebeu, C., Lake, J. A. 1982. *Proc.
   Natl. Acad. Sci. USA* 79: 3111
5. Berkovitch-Yellin, Z., Wittmann, H. G.,

Yonath, A. 1990. *Acta Crystallogr.* B46:
637
6. Deleted in proof
7. Brimacombe, R., Atmadja, J., Stiege,
   W., Schueler, D. 1988. *J. Mol. Biol.* 199:
   115
8. Clark, W., Leonard, K., Lake, J. 1982.
   Science 216: 999
9. Dabbs, E. 1987. *Mol. Genet. Life Sci.
   Adv.* 6: 61

10. Eisenstein, M., Sharon, R., Berkovitch-Yellin, Z., Gewitz, H.-S., Weinstein, S., et al. 1991. *Biochemie* In press
11. Frank, J., Verschoor, A., Radamaacher, M., Wagenknecht, T. 1990. See Ref. 17, pp. 107
12. Gewitz, H. S., Glotz, C., Piefke, J., Yonath, A., Wittmann, H. G. 1988. *Biochimie* 70: 645
13. Gilbert, W. 1963. *Cold Spring Harbor Symp. Quant. Biol.* 28: 287
14. Hansen, H., Volkmann, N., Piefke, J., Glotz, C., Weinstein, S., et al. 1990. *Biochim. Biophys. Acta* 1050: 1
15. Hardesty, B., Kramer, G., eds. 1986. *Structure, Function and Genetics of Ribosomes.* Heidelberg/New York: Springer Verlag
16. Hardesty, B., Picking W. D., Odom O. W. 1990. *Biochim. Biophys. Acta* 1050: 197
17. Hill, E. W., Dahlberg, A., Garrett, R. A., Moore, P. B., Schlesinger, D., Warner, J. R., eds. 1990. *The Ribosomes: Structure, Function and Evolution.* Washington, DC: Am. Soc. Microbiol.
18. Hope, H., Frolow, F., von Böhlen, K., Makowski, I., Kratky, C., et al. 1989. *Acta Crystallogr.* B45: 190
19. Jahn, W. 1989. *Z. Naturforsch.* 44b: 1313
20. Klug, A., Holmes, K. C., Finch, J. T. 1961. *J. Mol. Biol.* 3: 87
21. Kolb V. A., Kommer A., Spirin A. S. 1990. *FEBS Workshop on Translation, Leiden,* p. 84a
22. Kuhlbrandt, W., Unwin, P. N. T. 1982. *J. Mol. Biol.* 156: 611
23. Kurzchalia, S. V., Wiedmann, M., Bretcr, H., Zimmcrmann, W., Bauschke, E., Rapoport, T. A. 1988. *Eur. J. Biochem.* 172: 663
24. Lake, J. 1980. In *Ribosomes Structure, Function and Genetics.* ed. G. Chambliss, G. R. Craven, J. Davies, K. Davies, J. Kahan, N. Nomura, p. 207. Baltimore: Univ. Park Press
25. Leonard, K. R., Arad, T., Tesche, B., Erdmann, V. A., Wittmann, H. G., Yonath, A. 1982. In *Electron Microscopy 1982,* 3: 9. Hamburg: Offizin Paul Hartung
26. Makowski, I., Frolow, F., Saper, M. A., Wittmann, H. G., Yonath, A. 1987. *J. Mol. Biol.* 193: 819
27. Malkin, L. I., Rich, A. 1967. *J. Mol. Biol.* 26: 329
28. McPhearson, A., Koszelak, S., Axelrod, H., Day, J., Williams, R. 1986. *J. Biol. Chem.* 261: 1969
29. Milligan, R. A., Unwin, P. N. T. 1986. *Nature* 319: 693
30. Müssig, J., Makowski, I., von Böhlen, K., Hansen, H., Bartels, K. S., et al. 1989. *J. Mol. Biol.* 205: 619
31. Oakes, M., Henderson, E., Scheiman, A., Clark, M., Lake, J. 1986. See Ref. 15, pp. 47–67
32. Rheinberger, H.-J., Nierhaus, K. H. 1990. *Eur. J. Biochem.* 193: 643
33. Roth, M., Lewit-Bentley, A., Michel, H., Deisenhofer, J., Huber, R., Oesterheld, D. 1989. *Nature* 340: 659
34. Ryabova, L. A., Selivanova, O. M., Baranov, V. I., Vasiliev, V. D., Spirin, A. S. 1988. *FEBS Lett.* 226: 255
35. Trakhanov, S. D., Yusupov, M. M., Agalarov, S. C., Garber, M. B., Ryazantsev, S. 220: 319
36. Trakhanov, S. D., Yusupov, M. M., Shirokov, V. A., Garber, M. B., Mitschler, A., et al. 1989. *J. Mol. Biol.* 209: 327
37. Volkmann, N., Hottentrager, S., Hansen, H., Zayzsev-Bashan, A., Sharon, R., et al. 1990. *J. Mol. Biol.* 216: 239
37a. von Böhlen, K., Makowski, I., Hansen, H. A. S., Bartels, H., Berkovitch-Yellin, Z., et al. 1991. *J. Mol. Biol.* In press
38. Wagenknecht, T., Carazo, J. M., Radermacher, M., Frank, J. 1989. *Biophys. J.* 55: 455
39. Weinstein, S., Jahn, W., Wittmann, H. G., Yonath, A. 1989. *J. Biol. Chem.* 264: 19138
40. Deleted in proof
41. Wittmann, H. G., Müssig, J., Gewitz, H. S., Piefke, J., Rheinberger, H. J., Yonath, A. 1982. *FEBS Lett.* 146: 217
42. Yonath, A. 1984. *TIBS* 9: 227
43. Yonath, A., Bcnnctt, W., Wcinstein, S., Wittmann, H. G. 1990. See Ref. 17, p. 134
44. Yonath, A., Glotz, C., Gewitz, H. S., Bartels, K., von Böhlen, K., et al. 1988. *J. Mol. Biol.* 203: 831
45. Yonath, A., Khavitch, G., Tesche, B., Müssig, J., Lorenz, S., et al. 1982. *Biochem. Int.* 5: 629
46. Yonath, A., Leonard, K. R., Wittmann, H. G. 1987. *Science* 236: 813
47. Yonath, A., Müssig, J., Tesche, B., Lorenz, S., Erdmann, V. A., Wittmann, H. G. 1980. *Biochem. Int.* 1: 428
48. Yonath, A., Saper, M. A., Makowski, I., Müssig, J., Piefke, J., et al. 1986. *J. Mol. Biol.* 187: 633
49. Yonath, A., Wittmann, H. G. 1988. *Methods Enzymol.* 164: 95
50. Yonath, A., Wittmann, H. G. 1989. *TIBS* 14: 329